TECHNISCHE MECHANIK
European Journal of Engineering Mechanics
Diamond Open Access
journal homepage: www.ovgu.de/techmech

Tech. Mech., Vol. 46, Is. 1, (2026), 43–54
Received: 06.11.2025
Accepted: 08.01.2026
Available online: 16.02.2026

CFD modelling of the thermo- and hydrodynamic capabilities of long-necked plesiosaurs (Sauropterygia, Elasmosauridae)

Miguel Marx[1], Robert-Zoltán Szász[2⋆], and Johan Lindgren[1]

[1] Lund University, Department of Geology, Sölvegatan 12, SE-223 62 Lund, Sweden
[2] Lund University, Department of Energy Sciences, Ole Römersväg 1F, SE-223 63 Lund, Sweden

Abstract: Plesiosaurs are secondarily aquatic reptiles with a fossil record extending over 140 million years, and their fossilised remains have been found in sediments deposited in both warm, equatorial waters and cold, high-latitude environments. They are usually portrayed as a snake threaded through the body of a sea turtle. However, due to a general absence of preserved soft tissues, reconstructing the life appearance of particularly long-necked forms is anything but a straightforward task. Moreover, animals with such an oddly-shaped body form are unlikely to survive in cold-water environments. To investigate the ability of these ancient marine reptiles to inhabit high-latitude waters, we examined the heat transfer in two virtually reconstructed plesiosaurs: one built according to conventional wisdom (i.e., with a long and narrow neck) and one equipped with a peripheral layer of insulating blubber. We compared several modelling approaches (gradually increasing the complexity of our virtual reconstructions) to assess their pros and cons. We also investigated the temperature distribution within the two body types and tested their hydrodynamic performance by simulating a cruising plesiosaur at a steady velocity. The results of our endeavors show that insulating blubber must have been present to assure a suitable temperature distribution within the plesiosaur body when it inhabited cold water regions.

Keywords: blubber, heat transfer, plesiosaurs, temperature distribution

Nomenclature

c_p	[J/(kg K)]	specific heat at constant pressure
L	[m]	length
MR	[W/kg]	metabolic rate
R	[m]	radius
T	[K]	temperature
t	[s]	time
q	[W/m^3]	heat source
α	[m^2/s]	thermal diffusivity
κ	[W/(m K)]	heat conductivity
ϕ	[W/m^2]	heat flux per unit area
ρ	[kg/m^3]	density

1 Introduction

Palaeontology is an interdisciplinary science that integrates methods from various fields, including Computational Fluid Dynamics (CFD) Gutarra and Rahman (2022). From a CFD perspective, plesiosaurs – an iconic group of Mesozoic marine reptiles – have garnered some attention in recent years due to their distinctive morphology (long neck, turtle-like body, and four flippers), making them interesting subjects for numerical analyses Troelsen et al. (2019); Gutarra et al. (2022). While some investigations have been done on their swimming performance (see, e.g., Troelsen et al. (2019); Gutarra et al. (2022)), little is known about their thermodynamic capabilities. Notably, fossils of plesiosaurs have been recovered from high-latitude environments (Kubo et al. (2012); Rogov et al. (2019); Kear (2006)), to suggest that these animals were capable of surviving in cold water regimes, something that likely would have necessitated some sort of insulation. Their presence in high-latitude environments may also provide insight into the physiology of plesiosaurs.

The metabolism of plesiosaurs remains critically understudied. Historically, they were assumed to be ectothermic (cold-blooded) with relatively slow swimming speeds Hildebrand et al. (1930). In the late 20th century, however, this perception began to shift after a study by Wiffen et al. (1995), which represents an early attempt to indirectly infer metabolic strategies in plesiosaurs based on osteohistology. These authors interpreted the rapid apposition of periosteal bone as evidence of a sustained high metabolic rate. A major advance came in 2010 with the first geochemical approach to study plesiosaur physiology by Bernard et al. (2010), who analysed stable oxygen isotopes in teeth collected from Jurassic and Cretaceous strata. Their goal was to compare $\delta^{18}O$ values of various Mesozoic marine reptiles (including plesiosaurs) with those of contemporaneous fish (which principally are ectothermic). Since in ectotherms, compared to endotherms (warm-bloodied animals), $\delta^{18}O$ values should be

⋆ E-mail address: robert-zoltan.szasz@energy.lth.se doi: 10.24352/UB.OVGU-2026-006 2026 | All rights reserved.

higher in high-latitude environments (cold climates) Amiot et al. (2006), the lower amounts of $\delta^{18}O$ (compared to the associated fish 'standards') in the plesiosaur samples investigated by Bernard et al. (2010) indicated an endothermic metabolism according to these authors (figs. 1 and 2 in Bernard et al. (2010)).
After Bernard et al. (2010), several geochemical and histological studies have supported the hypothesis of an elevated metabolism in plesiosaurs Wintrich et al. (2017); Fleischle et al. (2018); Wiemann et al. (2022); Séon et al. (2024); Sambuichi et al. (2025).
For instance, a histological analysis by Wintrich et al. (2017) of the earliest known plesiosaur, *Rhaeticosaurus mertensi*, indicated exceedingly fast growth, as evidenced by the presence of fast-growing radial fibro-lamellar bone tissue, to suggest that even the earliest forms were endothermic. This interpretation was subsequently corroborated by Fleischle et al. (2018), who found plesiosaurs to have an exceptionally high metabolism, comparable to that of modern birds. Raman and Fourier-transform infrared spectroscopy of metabolic lipoxidation products preserved in fossil bone further indicate endothermy in plesiosaurs Wiemann et al. (2022). Recent stable oxygen isotope analyses by Séon et al. (2024) and Sambuichi et al. (2025) suggest that plesiosaurs were facultative endotherms or regional endotherms; i.e., capable of elevating their metabolism close to endothermic levels. Although it remains inconclusive whether plesiosaurs were strictly homeothermic endotherms (capable of maintaining a high body temperature) or poikilothermic (body temperature varies depending on the environment), it is reasonable to hypothesize that they could likely reach metabolic rates comparable to those of endothermic animals.
CFD offers an additional approach to test plesiosaur metabolic strategies by assigning either ectothermic or endothermic heat-generating regions to a 3D plesiosaur model, and measuring heat distribution in a simulation that mimics a plesiosaur submerged in water. Using this method, we can directly test whether a plesiosaur could survive various ocean temperatures, derived from paleotemperature data, under different metabolic scenarios.
Modern whales and even a species of sea turtle (*Dermochelys coriacea*; the leatherback turtle) utilize a combination of high metabolism, large body size and blubber (a peripheral insulating tissue) to resist the effects of cold water Paladino et al. (1990); Fish (2000). Blubber was apparently also present in at least some derived ichthyosaurs, another group of extinct marine reptiles Lindgren et al. (2018). Thus, we hypothesize that plesiosaurs likewise employed some sort of peripheral tissue layer to enable life in cold-water environments.
Modelling heat transfer in an animal poses a number of challenges. To start with, there are several body regions (e.g., muscle, brain) where heat production is hard to assess. The heat conductivity of tissues is also difficult to measure accurately, and the circulatory system that regulates heat transfer between different body parts is likewise challenging to model Hokkanen (1990). Furthermore, given that plesiosaurs are extinct, the required parameters have to be estimated from living animals.
Several models are available to replicate the physical phenomena involved in heat transfer processes. However, increasing the level of detail also amplifies model complexity, which in turn raises both the computational requirements and the human effort needed to set up and analyze the cases. Moreover, when multiple parameters remain unknown, a more complex model does not necessarily yield better results.
One of the goals of this study is to compare modeling approaches at different levels of complexity to simulate a plesiosaur inhabiting a cold-water environment. Additionally, by comparing a model based on the conventional reconstruction of the body shape to one equipped with an additional blubber layer, we evaluate the impact of additional insulation on temperature distribution and the associated drag penalties. Several metabolic-rate scenarios are investigated, ranging from levels typical of passive animals to those characteristic of intensely exercising ones.

2 Methods

2.1 One-dimensional analysis

The simplest model assumes that the blubber layer is thin relative to the skin's surface area. Under this presumption, heat transfer through the blubber can be considered one-dimensional and thus evaluated using Fourier's law of heat conduction (Eq. 1). Fourier's law can, for example, be applied to estimate heat flux if the thermal conductivity, blubber thickness, and the temperature difference between the surrounding environment and the inner body temperature are known.

$$\phi = -\kappa \frac{\Delta T}{\Delta x} \tag{1}$$

For this initial model, blubber thickness and thermal conductivity values for various whale species were adapted from Hokkanen (1990) and Dunkin et al. (2005) and references therein. Blubber thickness for the leatherback turtle was obtained from Wyneken (2015), and its thermal conductivity was assumed to be 0.3 $\mathrm{W/(m\,K)}$, based on the work of Kvadsheim et al. (1996) and Dudley et al. (2016). The thermal conductivity of human fat was taken from Dunkin et al. (2005) and the thickness was assumed to be 1 centimeter Störchle et al. (2018).

2.2 Cylindrical model

Due to their overall elongated body form, the heat-transfer characteristics of several marine animals were investigated by assuming a cylindrical shape. For example, Hokkanen (1990) examined the temperature regulation of marine mammals using this model. By neglecting end effects, heat transfer can be evaluated in a single (radial) direction. This model has the advantage of accounting for both volume and surface-area effects compared to the one-dimensional model presented in the previous subsection. Here, we estimated the heat flux across a blubber layer with inner radius R_{in} and outer radius R_{out} for an animal of length L, using Eq. 2 Cengel (2004).

$$Q = 2\pi\kappa L \frac{\Delta T}{\ln(R_{\text{out}}/R_{\text{in}})} \tag{2}$$

The heat flux was calculated using body dimensions of the modern right whale (*Eubalaena*, Hokkanen (1990); Christiansen et al. (2020)), harbour porpoise (*Phocoena phocoena*, Hokkanen (1990); Read et al. (2025)), leatherback turtle (Wyneken (2015); Price et al. (2004)), and two plesiosaur models: one with a thin (1 cm) blubber layer and another with a thicker (7 cm) layer. The total length of the plesiosaur cylindrical model was set to 11.7 m, based on a reconstruction of the extremely long-necked elasmosaurid, *Albertonectes vanderveldei* (TMP 2007.011.0001: Tyrell Museum of Paleontology, Drumheller, Alberta, Canada) Kubo et al. (2012).

2.3 3D heat conduction

Heat conduction in an arbitrary three-dimensional geometry, which may include internal heat sources, can be investigated by solving the Poisson equation (Eq. 3). For this purpose, the laplacianFoam solver implemented in OpenFOAM v2306 was used.

$$\frac{\partial T}{\partial t} = \nabla \cdot (\alpha \nabla T) + \frac{q}{\rho\, c_p} \tag{3}$$

Two plesiosaur geometries, based on *Albertonectes vanderveldei*, were constructed using FreeCAD: one without blubber and another coated with an insulating layer (based on the actual blubber thickness of the leatherback turtle, as reported by Wyneken (2015)). The total length of each geometry was set to 11.7 m. The thickness of muscle tissue encasing the skeleton was approximated from comparisons with modern reptiles Cieri (2018); Klingler (2016); Davenport et al. (2009). In the blubber-coated model, this peripheral tissue was applied to all body regions except the flippers. Figure 1 shows a perspective view of the reconstructed geometry without blubber (left) and with blubber (right).
The thermal conductivity of blubber (≈ 0.30 W/(m K)) is significantly lower than that of muscle tissue (≈ 0.57 W/(m K)) Hokkanen (1990); therefore, it is important to investigate the impact of regions with different thermal conductivities on the resulting thermal balance. Furthermore, the heat source in this case is metabolic, depending on the animal's activity level Bostrom and Jones (2007).
In addition to the magnitude of the metabolic rate, the spatial extent of the region where heat is generated is also important. The simplest assumption is uniform heat release throughout the body. However, in reality, heat generation varies across different body regions Grayson et al. (1966); Block (1994). To investigate the impact of heat-release zone size, a third geometry was created to include a simplified viscera (internal organs), major arteries, and a brain — collectively referred to as the 'organ region' for simplicity. Figure 2 visualizes this organ region (green), the muscle region (red), and the added blubber layer (light blue). The two black circles in the brain and torso regions mark the locations where temperature is monitored for post-processing. Dividing the geometry into multiple regions primarily affects the mesh-generation process. At the interface between regions, internal boundaries (called 'baffles' in OpenFOAM terminology) are introduced. Our mesh is refined in these regions to better resolve temperature gradients. From the solver's perspective, the entire mesh remains a single computational domain; the regions exist solely to assign different material properties.

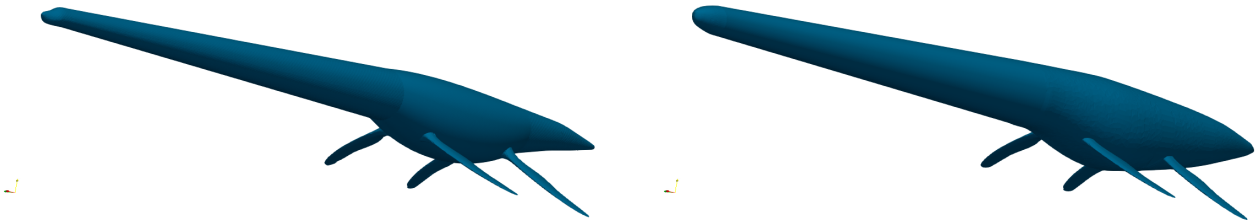

Fig. 1: Perspective view of the adopted plesiosaur geometry without (left) and with (right) blubber.

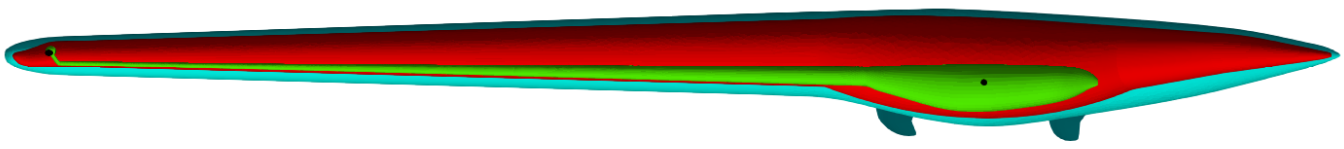

Fig. 2: Side view of the adopted plesiosaur geometry, showing the internal organ region in green, the outer muscle region in red, and the added blubber layer in light blue. The black circles indicate the locations of the monitoring points.

Tissues in the geometries were assigned thermal conductivity values reported for extant marine animals: muscle and organ regions (0.57 W/(m K), Hokkanen (1990)), and blubber (0.30 W/(m K), Dunkin et al. (2005); Bostrom and Jones (2007)). In certain cases, the thermal conductivity of blubber was adjusted to 0.57 W/(m K) to replicate vasodilation of the circulatory system within

the blubber tissue, since this is a known physiological adaptation for cooling in marine animals Dudley et al. (2016); Hokkanen (1990); Paladino et al. (1990). A specific heat capacity of 3.75 kJ/(kg K) was applied to all tissues Bostrom and Jones (2007).

Paladino et al. (1990) investigated the metabolic rate of leatherback turtles by analyzing oxygen and carbon dioxide concentrations, breathing rate, and the volume of expired air. Thus, the metabolic rates reported by Paladino et al. (1990) reflect whole body metabolism; the values of which were adopted for our plesiosaur models. Here, three different metabolic rates were assigned to the models: a lower rate ($MR = 0.083$ W/kg) Bostrom and Jones (2007); Lutcavage et al. (1990), corresponding to an inactive, cold-blooded animal, an elevated rate ($MR = 1.51$ W/kg), typical of a leatherback turtle during intense activity (see Paladino et al. (1990)), and a moderate rate ($MR = 0.8$ W/kg), which is close to the lower end of the high metabolic rate range reported by Paladino et al. (1990), and is approximately the average of the adopted extreme values.

The heat-generating regions were assigned either to the entire body or exclusively to the organ region. No metabolic rate was assigned to the blubber, as we assume it to be a non-heat-generating tissue Tian et al. (2025).

A water temperature of 285.15 K (12 °C) was chosen because it approximates conditions experienced by *A. vanderveldei* based on clumped oxygen isotope analysis by Petersen et al. (2016) at a depth of 25 meters. Prescribing the water temperature directly on the skin neglects the thermal boundary layer formed in the water near the body. As a consequence, the cooling effect of the water is overpredicted. Nevertheless, according to Hokkanen (1990), the associated error is likely small.

The Gauss linear scheme was used to discretize the temperature gradient, and the Gauss linear corrected scheme for the Laplacian. The solver is based on the Preconditioned Conjugate Gradient (PCG) method with a Diagonal-based Incomplete Cholesky (DIC) preconditioner. For details on discretization and solution methods, see the OpenFOAM documentation. The initial temperature of the model was set equal to the water temperature (285.15 K). The computations were run until steady-state conditions were achieved; i.e., until the residuals stabilized at a constant level.

2.4 Hydrodynamic force computations

In addition to heat balance, an added blubber layer influences the hydrodynamic forces acting on the body. To estimate this impact, two additional simulations were performed. The flow around the two plesiosaur geometries was solved using the simpleFoam solver in OpenFOAM v2306. Pressure–velocity coupling was based on the SIMPLE algorithm (see, e.g., Versteeg and Malalasekera (2007)). The computational domain extended from (−40 m, −25 m, −25 m) to (100 m, 25 m, 25 m) (Figure 3), with the model located at $(0, 0, 0)$. The k–ω SST turbulence model reported by Menter and Esch (2001) and Menter et al. (2003) was employed. The inlet velocity magnitude was set to 1.5 m/s, approximating the estimated cruising speed of other extinct marine reptiles Motani (2002). The computational domain was considered sufficiently long to avoid flow reversal at the outlet. Nevertheless, to ensure robustness, the outlet boundary was specified as inletOutlet. This condition acts as an outlet (fixed pressure, zero gradient for velocity) when flow exits the domain, and as an inlet (fixed velocity, zero gradient for pressure) in case of flow reversal. On the plesiosaur body surface, a no-slip condition was applied for velocity, zero gradient for pressure, and wall functions for turbulent kinetic energy (k) and specific dissipation rate (ω). The side walls of the computational domain were treated as slip boundaries. A grid-sensitivity study with meshes of 1.2, 3.0, 9.1, and 31.4 million cells indicated that 9.1 million cells provided a good balance between accuracy and computational cost. This mesh was obtained in three steps. First, an equidistant cartesian mesh was generated containing 56×20×20 cubic cells with 2.5 m edges. Next, the mesh was refined by applying ten levels of oct-tree refinements. Finally, two layers of boundary cells were added with an expansion ratio of 1.3. The resulting mesh is hex-dominant (87%), non-hexahedral cells being generated only in the vicinity of solid surfaces. The reported average y^+ value for this resolution was 28.7 (minimum: 0.6; maximum: 155).

3 Results

3.1 One-dimensional analysis

The effects of blubber thickness and its thermal conductivity are clearly illustrated in Figure 4. The temperature difference to the surroundings was set to 25 K. The relatively thin layer of fat in humans allows for a higher heat flux compared to fluxes predicted for cetaceans, which possess both thicker blubber and lower thermal conductivity values. Notably, a plesiosaur inhabiting cold-water environments would benefit from having a peripheral layer of insulating blubber.

3.2 Cylindrical model

Using Eq. 2, the total heat flux was estimated for two versions of the modeled plesiosaur (one with and one without blubber), as well as for several extant tetrapods for comparison. The adopted parameters and estimated heat fluxes for an assumed temperature difference of $\Delta T = 25$ K are summarized in Table 1.

A right whale (a species well adapted to cold waters), at approximately the same length as our modeled plesiosaur (≈ 12 m), but with greater volume and blubber thickness, exhibits a significantly lower heat flux compared to the plesiosaur without blubber. Adding a 7 cm blubber layer (similar to that of an adult leatherback turtle) to the plesiosaur model significantly reduces the heat flux to a magnitude comparable to the other species considered. This reduction suggests that plesiosaurs would have benefited from an insulating blubber layer.

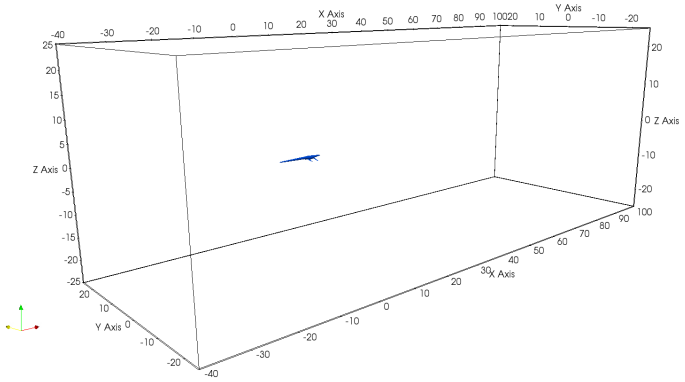

Fig. 3: Computational domain used for flow simulations.

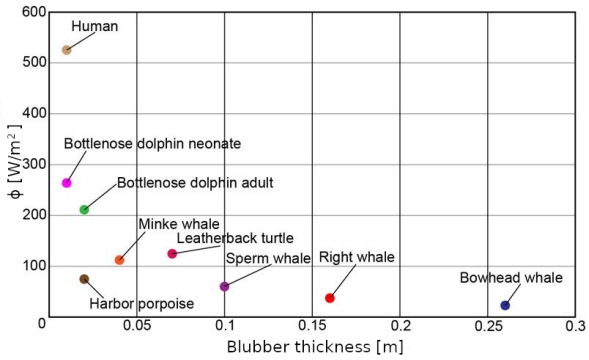

Fig. 4: Predicted heat flux values for selected extant tetrapods.

Tab. 1: Heat flux predicted for plesiosaurs and selected modern animals.

Animal	R_{out} [m]	R_{in} [m]	L [m]	κ [W/(m K)]	Q [W]
Harbour porpoise	0.08	0.06	1.6	0.1	87
Right whale	1.17	1.01	12	0.3	3845
Leatherback turtle	0.52	0.45	2	0.3	652
Plesiosaur (no blubber)	0.43	0.42	11.7	0.3	23431
Plesiosaur (blubber)	0.49	0.42	11.7	0.3	3577

3.3 Three-dimensional heat transfer calculations

The purpose of these computations was to investigate temperature distribution within the plesiosaur body under various scenarios. In all simulations, the water temperature was set to 285.15 K (12 °C). Moreover, based on experiments on hatchling sea turtles reported by Schwartz (1978), we make the assumption that the lowest body temperature a plesiosaur could comfortably tolerate is 288.15 K (15 °C), while the highest is 313.15 K (40 °C). Hence, the color scales in the following figures span the 285.15–313.15 K interval (i.e., 12–40 °C). Optimal temperatures correspond to regions colored either dark blue or red.

Two critical regions were considered: first, the long and narrow neck, where water might cool the brain to dangerously low temperatures; second, the torso, which has a low surface-area-to-volume ratio and may therefore be prone to overheating.

We investigated the impact of key parameters–such as metabolic rate, thermal conductivity, and the presence of a peripheral blubber layer–on body temperature distribution. Additionally, a three-region case was set up to model the effects of enhanced heat transfer due to an introduced circulatory system, albeit in a simplified manner.

3.3.1 Influence of metabolic rate magnitude

The influence of metabolic rate on temperature distribution was evaluated using a model without blubber. The two extreme cases correspond to an inactive individual (MR = 0.083 W/kg) and a highly active animal (MR = 1.51 W/kg). The moderate case (MR = 0.80 W/kg) is approximately the average of the extreme values and close to the lowest metabolic rate reported by Paladino et al. (1990) for exercising adult leatherback turtles. In all cases, the heat source was restricted to the organ region (green in Fig. 2), and thermal conductivity was set to 0.57 W/(m K). In the low-activity case (Fig. 5a), body temperatures are suboptimal, with the head and neck nearly matching the surrounding water temperature. It is highly unlikely that a plesiosaur could have survived under such conditions for an extended period of time. With increasing metabolic rates, temperatures rise toward optimal levels in the brain region (286.1 K in the moderate case and 287.0 K in the high-rate case). In the torso region, the temperature at the monitoring point exceeds survivable levels in the moderate case (317.8 K) and reaches an even higher value (346.8 K) in the high-rate case.

3.3.2 Influence of heat source region

The amount of heat generated in different body parts varies, depending on factors such as the animal's activity level. Since quantifying heat generation in different parts of an extinct animal is challenging, we present a sensitivity study illustrating two extreme conditions: heat generated only in the organ region (green in Fig. 2) or throughout the entire body (green and red regions in Fig. 2). Figure 5 shows temperature distribution for various metabolic rates when heat is generated only in the organ region. Figure 6 presents the predicted temperature distribution for the same metabolic rates when heat is assumed to be generated throughout the entire body. As expected, body temperature levels increase when heat sources are distributed throughout the entire body. Consequently, for the low metabolic rate case, torso temperatures approach ideal values (297.9 K), while brain temperature remains too low (285.9 K). For higher metabolic rates, brain temperature becomes more suitable for survival (288.8 K, 292.1 K), but large portions of the body overheat, with the torso monitoring point reaching 350.0 K and 407.6 K, respectively.

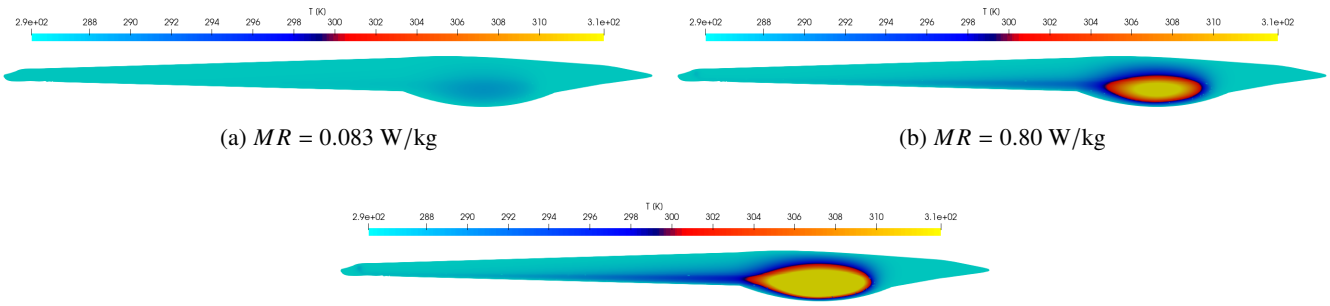

(a) $MR = 0.083$ W/kg (b) $MR = 0.80$ W/kg

(c) $MR = 1.51$ W/kg

Fig. 5: Temperature distribution in a plesiosaur model without blubber at low (a), medium (b), and high (c) metabolic rates ($\kappa = 0.57$ W/(m K)), with heat source restricted to the organ region.

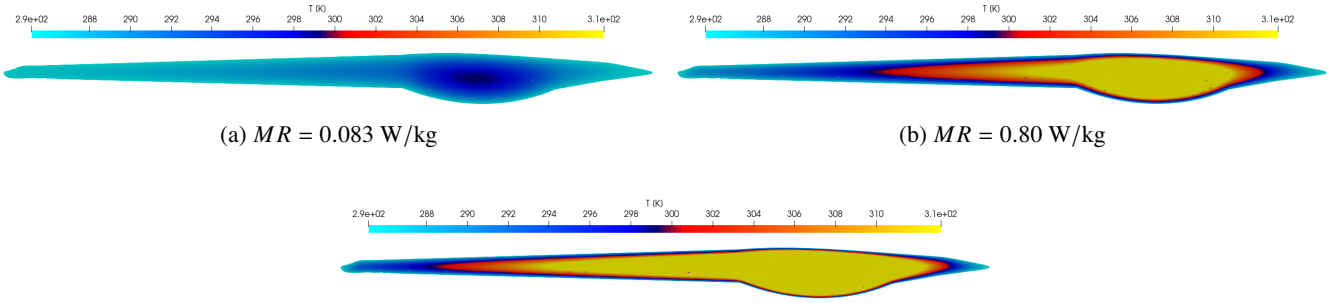

(a) $MR = 0.083$ W/kg (b) $MR = 0.80$ W/kg

(c) $MR = 1.51$ W/kg

Fig. 6: Temperature distribution in a plesiosaur model without blubber at low (a), medium (b), and high (c) metabolic rates ($\kappa = 0.57$ W/(m K)), with heat source distributed throughout the entire body.

3.3.3 Influence of thermal conductivity

Thermal conductivity can vary not only between tissues but also within the same tissue, depending, for example, on circulatory system effects. Three values were considered: the lowest ($\kappa = 0.30$ W/(m K)), typical for blubber (see Kvadsheim et al. (1996)); the second ($\kappa = 0.57$ W/(m K)), representative of muscle tissue; and the third ($\kappa = 2.00$ W/(m K)), adopted to mimic enhanced heat transfer by convection effects due to the circulatory system.

Figure 7 shows temperature distribution for the lowest metabolic rate case ($MR = 0.083$ W/kg). As expected, higher thermal conductivity values lead to more uniform heat distribution and a stronger cooling effect. The predicted brain temperature decreases from 285.34 K ($\kappa = 0.30$ W/(m K)) to 285.25 K ($\kappa = 0.57$ W/(m K)), and finally to 285.18 K ($\kappa = 2.00$ W/(m K)). The torso region also cools from 291.6 K ($\kappa = 0.30$ W/(m K)) to 286.1 K (for $\kappa = 2.00$ W/(m K)).

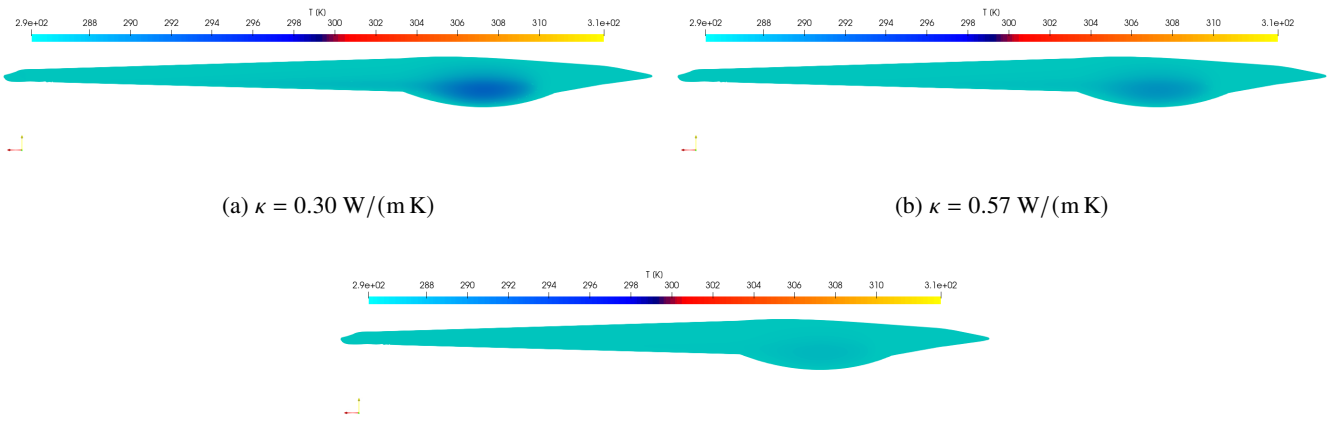

(a) $\kappa = 0.30$ W/(m K) (b) $\kappa = 0.57$ W/(m K)

(c) $\kappa = 2.00$ W/(m K)

Fig. 7: Impact of thermal conductivity on temperature distribution in a plesiosaur without blubber ($MR = 0.083$ W/kg).

3.3.4 Influence of blubber

The temperature distribution of a plesiosaur model, covered by an external blubber layer, was analyzed for several metabolic rates and thermal conductivity values. Figure 8 illustrates four distinct parameter combinations. In all scenarios, heat is generated throughout the body, apart from the blubber layer.

Figure 8a shows the temperature distribution for a low metabolic rate case. Here, thermal conductivities are typical of muscle and blubber tissues. Compared to the corresponding setup without blubber (Fig. 7b), temperatures are noticeably more favorable in most body regions. The torso temperature (295.6 K) falls within the optimal range; however, the predicted brain temperature (286.2 K) remains too low for comfort.

In the second case (Fig. 8b), blubber thermal conductivity is increased to 0.57 W/(m K). This condition could mimic, for example, improved heat transfer due to vasodilation. As expected, a stronger cooling effect occurs, with torso temperature dropping to 293.9 K, though still more viable than in the case without blubber (Fig. 7b).

The third case is characterized by a moderate metabolic rate (MR = 0.80 W/kg, Fig. 8c). Even with blubber thermal conductivity set to higher values (typical of muscle), and thus assuming more intense cooling, predicted temperatures remain excessively high (369.0 K in the torso), suggesting that the analyzed metabolic rate is too high. Temperatures in the highest metabolic rate case (MR = 1.51 W/kg, Fig. 8d) reach even more extreme values.

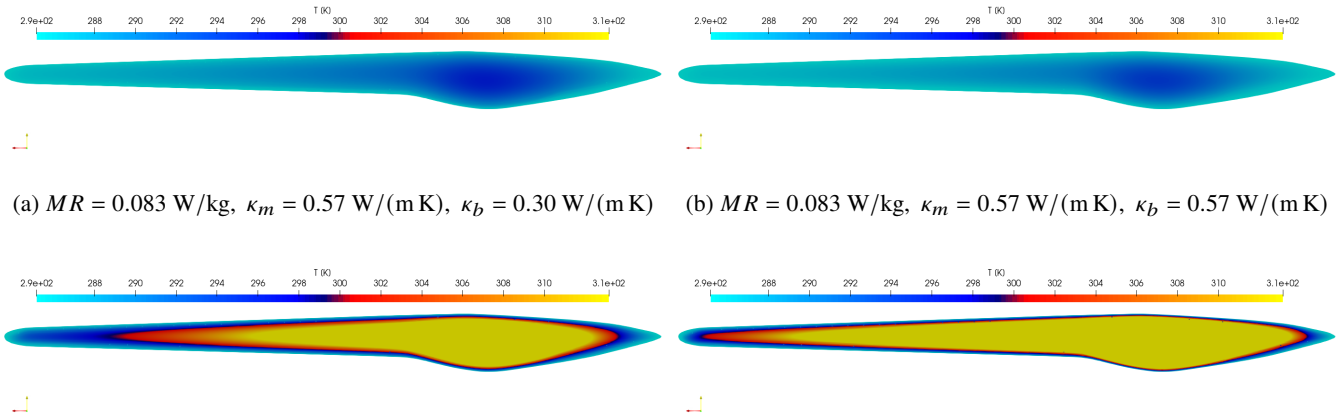

(a) MR = 0.083 W/kg, κ_m = 0.57 W/(m K), κ_b = 0.30 W/(m K)

(b) MR = 0.083 W/kg, κ_m = 0.57 W/(m K), κ_b = 0.57 W/(m K)

(c) MR = 0.80 W/kg, κ_m = 0.57 W/(m K), κ_b = 0.57 W/(m K)

(d) MR = 1.51 W/kg, κ_m = 0.57 W/(m K), κ_b = 0.57 W/(m K)

Fig. 8: Impact of blubber layer on temperature distribution.

3.3.5 Impact of the circulatory system

Heat transfer by blood convection is a typical process to redistribute heat in animals, yet challenging to model accurately. Because of the wide range of scales involved, an explicit computation—even if limited to the larger vessels—would be computationally prohibitive. Therefore, we adopted a simplified approach, representing convective heat transfer through an increased effective thermal conductivity coefficient. Following Hokkanen (1990), realistic blood flow rates lie between 1–4 kg/(m^3 s), corresponding to heat transfer rates of approximately 4000–16000 W/(m^3 K). By dimensional analysis, the chosen conductivity (κ = 2 W/(m K)) implies cross-sectional areas of 125–500 mm^2, which are reasonable given the animal's size (torso diameter ≈ 1 m).

For this study, the computational domain was divided into three regions (see Figure 2): the outermost region represents blubber (κ = 0.30 W/(m K)), the middle region represents muscle (κ = 0.57 W/(m K)), and the innermost region (organ region) was assigned a higher thermal conductivity to mimic enhanced heat transfer (κ = 2 W/(m K)). Two metabolic rates were considered: moderate (MR = 0.8 W/kg) and high (MR = 1.51 W/kg). Heat generation was restricted to the organ region of the body. The resulting temperature distributions are presented in Figures 9a and 9b.

Compared to the blubber cases predicted with a two-zone model (Fig. 8), the temperatures obtained using the three-region configurations are lower. Since the two- and three-region models differ not only in the thermal conductivity of the inner organ zone but also in the spatial extent of the heat source region, two additional configurations were tested for the high metabolic rate case. Figure 9c shows the temperature distribution when the thermal conductivity of the organ region is reduced from 2.0 W/(m K) to 0.57 W/(m K). As expected, the predicted temperatures increase; however, the changes are relatively modest: brain temperature rises from 287.2 K to 287.7 K, while torso temperature increases from 339.5 K to 361.7 K. When the heat source region is extended to the entire body (excluding the blubber), the resulting temperature distribution is shown in Figure 9d. It is evident that the extent of the heat release zone has a substantially greater impact on predicted temperatures, which reach 304.3 K and 475.2 K in the brain and torso regions, respectively.

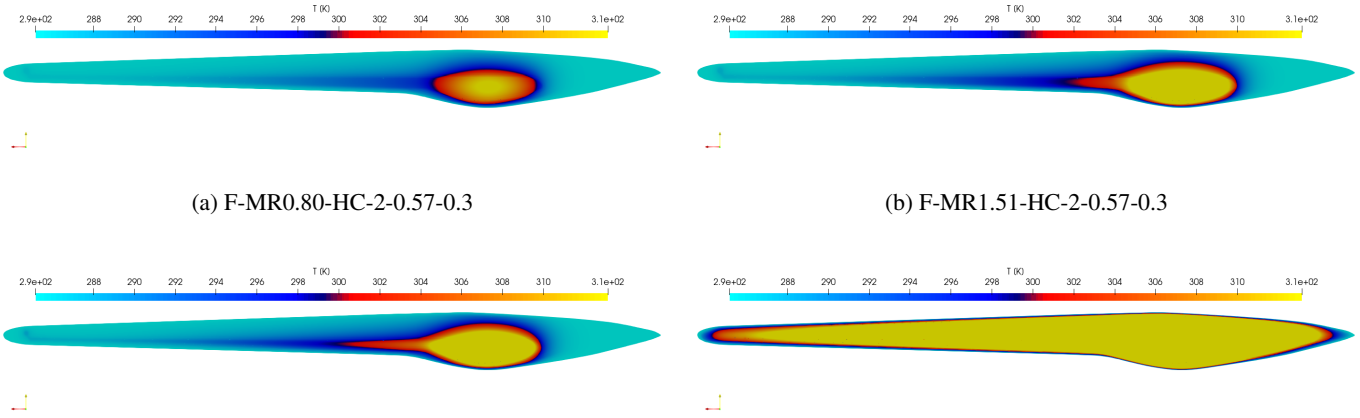

(a) F-MR0.80-HC-2-0.57-0.3

(b) F-MR1.51-HC-2-0.57-0.3

(c) F-MR1.51-HC-0.57-0.57-0.3

(d) F-MR1.51-HC-0.57-0.57-0.3-A

Fig. 9: Temperature distributions for selected cases predicted using three regions. See Table 2 for the case parameters.

3.3.6 Summary of the three-dimensional cases

For a quantitative comparison, temperatures at monitoring points in the brain and torso regions are summarized in Table 2 and visualized in Figure 10. For reference, the inferred minimum and maximum viable temperature thresholds are also shown. Several cases exhibit torso temperatures within viable limits, whereas only three cases yield brain temperatures suitable for survival. In those cases, however, torso temperatures substantially exceed the upper allowable limit. Other scenarios show brain temperatures near the lower limit. With more accurate modeling of the circulatory system effects, both brain and torso temperatures could fall within viable ranges.

Tab. 2: Summary of the three-dimensional cases

Case	Blubber	Metabolic rate $[\frac{\mathrm{W}}{\mathrm{kg}}]$	Heat conductivity $[\frac{\mathrm{W}}{\mathrm{m\,K}}]$	Heat source region	Brain temperature [K]	Torso temperature [K]
S-MR0.08-HC0.30	No	0.083	0.3	organ	285.3	291.6
S-MR0.08-HC0.57	No	0.083	0.57	organ	285.2	288.5
S-MR0.08-HC0.57-A	No	0.083	0.57	all	285.9	297.9
S-MR0.08-HC2.00	No	0.083	2	organ	285.2	286.1
S-MR0.80-HC0.57	No	0.80	0.57	organ	286.1	317.8
S-MR0.80-HC0.57-A	No	0.80	0.57	all	188.8	350.0
S-MR1.51-HC0.30	No	1.51	0.3	organ	288.6	401.9
S-MR1.51-HC0.57	No	1.51	0.57	organ	297.0	346.8
S-MR1.51-HC0.57-A	No	1.51	0.57	all	292.1	407.6
S-MR1.51-HC2.00	No	1.51	2	organ	285.7	302.7
F-MR0.08-HC0.57-0.30	Yes	0.083	0.57, 0.3	exc. blubber	286.2	295.6
F-MR0.08-HC0.57-0.57	Yes	0.083	0.57, 0.57	exc. blubber	285.9	293.9
F-MR0.80-HC0.57-0.57	Yes	0.80	0.57, 0.57	exc. blubber	292.3	369.0
F-MR1.51-HC0.57-0.57	Yes	1.51	0.57, 0.57	exc. blubber	298.6	443.5
F-MR0.80-HC-2-0.57-0.3	Yes	0.80	2, 0.57, 0.3	organ	286.2	313.9
F-MR1.51-HC-2-0.57-0.3	Yes	1.51	2, 0.57, 0.3	organ	287.2	339.5
F-MR1.51-HC-0.57-0.57-0.3	Yes	1.51	2, 0.57, 0.3	organ	287.7	361.7
F-MR1.51-HC-0.57-0.57-0.3-A	Yes	1.51	0.57, 0.57, 0.3	exc. blubber	304.3	475.2

Models with greater complexity require longer computation times. Table 3 summarizes typical convergence times when running 16 parallel processes on an AMD Ryzen 9 7950X3D, a 16-core processor. As expected, execution time increases markedly with finer mesh resolution. In addition, higher thermal conductivity values accelerate convergence, indicating that longer timesteps could have been applied in the lower-conductivity cases. Overall, the required computing times remain relatively short compared to more complex CFD simulations, and the effect of suboptimal timestep selection is considered negligible.

3.4 Flow computations

These computations were conducted to assess the effect of an added blubber layer on hydrodynamic drag. Figure 11 illustrates the pressure distribution along the surfaces of the original (left) and blubber-coated (right) geometries. Velocity magnitudes around both bodies are shown in Figure 12. No significant differences are evident in either pressure or velocity distributions. This

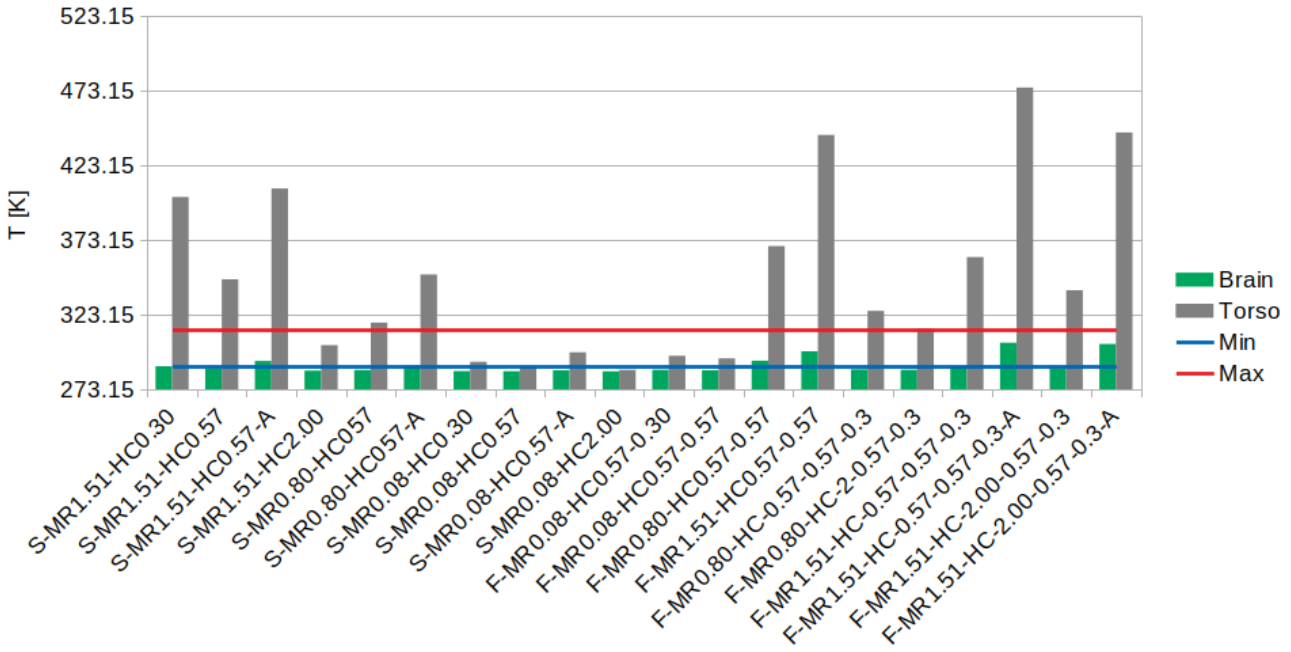

Fig. 10: Summary of observed temperatures at monitoring points in the brain and torso regions. Labels on the horizontal axis indicate each case: *S* denotes cases without blubber, *F* those with an additional blubber layer. The number following *MR* represents the metabolic rate, while values after *HC* indicate thermal conductivities.

Tab. 3: Typical CPU times.

Case type	MR $[\frac{\mathrm{W}}{\mathrm{kg}}]$	κ $[\frac{\mathrm{W}}{\mathrm{m\,K}}]$	N_{cells} $[\cdot 10^6]$	t_{conv} [s]
No blubber	1.58	0.30	1.9	509
No blubber	1.58	0.57	1.9	314
No blubber	1.58	2.00	1.9	134
No blubber	0.083	0.30	1.9	430
No blubber	0.083	0.57	1.9	307
No blubber	0.083	0.30	1.9	137
With blubber	1.51	0.57 0.57	3.8	5260
With blubber	0.83	0.57 0.30	3.8	6434
With blubber	0.83	0.57 0.57	3.8	5496
Three regions	1.51	2.0 0.57 0.25	16.2	35036

similarity is quantitatively confirmed by only a slight (1%) increase in drag force, from 100.92 N (original geometry) to 101.93 N (with blubber). Such a minor increase indicates that adding blubber does not impose a meaningful penalty on the hydrodynamic performance of the selected body shapes.

4 Discussion and summary

The impact of an added blubber layer on the heat balance of a plesiosaur was investigated using numerical models of varying complexity. Simple one-dimensional and cylindrical models indicated the necessity of an additional insulating layer to reduce simulated heat fluxes to levels comparable to those observed in modern tetrapods inhabiting or migrating in cold water for extended periods of time.

Three-dimensional computations further demonstrated that a peripheral insulating layer was essential for maintaining viable internal body temperatures. Without insulation, the predicted internal temperatures were lethally low at low metabolic rates, whereas high metabolic rates produced unrealistically high core temperatures. Despite this, the elongated neck caused brain-region temperatures to remain below survival thresholds in most cases.

Adding a blubber layer significantly improved thermal viability for individuals with low metabolic rates. However, for highly active animals, the added insulation amplifies overheating in the torso region, which suggests that the blubber thickness was likely variable and thinner in certain body regions.

Several uncertainties affect these predictions. To start with, there is no universally accepted plesiosaur body shape; our geometry is a simplified representation based on a real specimen Kubo et al. (2012). The thermophysical properties of tissues were approximated using data from modern animals, which vary between organs and even within the same tissue type Ouchi et al. (2021); Stoner (1973); Kiyatkin (2019). Nevertheless, our sensitivity analysis employed realistic extreme values, so actual conditions are expected to fall within the predicted range. Our computations predicted a significant impact of the extent of the heat release zone on the

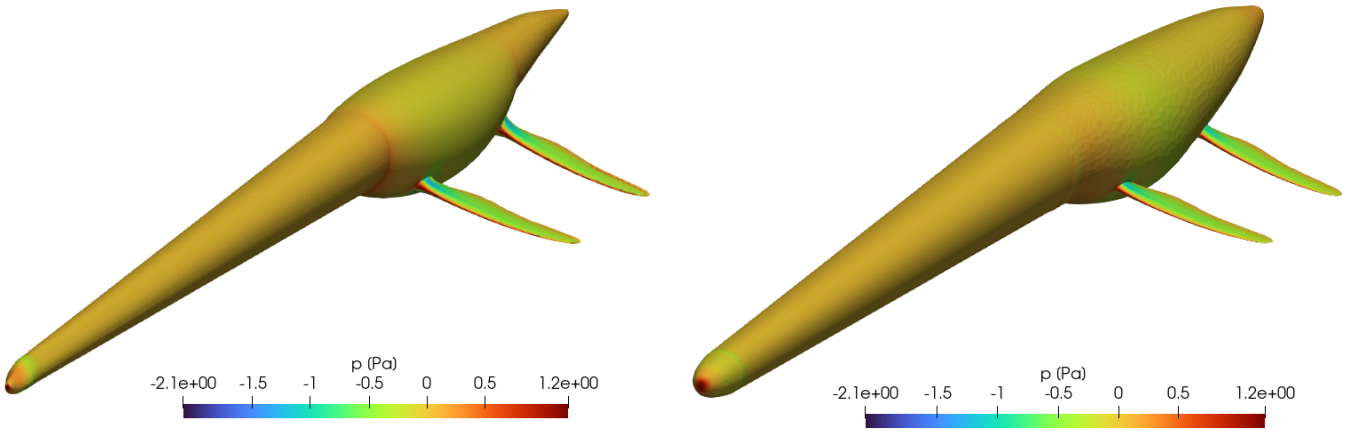

(a) Without blubber (b) With blubber

Fig. 11: Pressure distribution along the body: (a) without blubber and (b) with blubber.

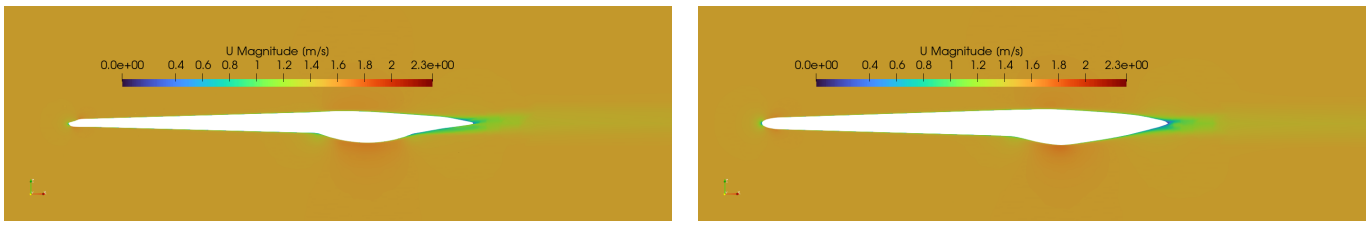

(a) Without blubber (b) With blubber

Fig. 12: Velocity distribution in a longitudinal cross-section: (a) without blubber and (b) with blubber.

temperature distribution. Therefore, a more accurate model would require multiple heat-generation zones with varying magnitudes, but such data are currently scarce. Another limitation is the treatment of convective heat transfer by blood flow. While a simplified approach was adopted, advanced vascular modeling (similar to the one reported by Wéber et al. (2023)) could be combined with OpenFOAM to allow the inclusion of further details. Finally, the assumption of a constant temperature boundary condition may overestimate cooling by the surrounding water. Although the literature suggests that this effect is minor, future work using conjugate heat transfer could verify whether this is the case or not.

Despite these unavoidable uncertainties, our results strongly suggest that the widely accepted plesiosaur body shape should be refined to include at least a peripheral blubber layer. Furthermore, the temperature distributions associated with the moderate metabolic rate, being closest to optimal values, suggest that the animals likely maintained a relatively high metabolic rate either through an endothermic strategy or via behavioral adaptations (for example sustained activity, as observed in leatherback turtles).

Acknowledgements

The computations were enabled by resources provided by the National Academic Infrastructure for Supercomputing in Sweden (NAISS), which is partially funded by the Swedish Research Council through grant agreement no. 2022-06725. Additional financial support was provided by a project grant (no. 2020-03542) from the Swedish Research Council awarded to Johan Lindgren.

References

R. Amiot, C. Lécuyer, E. Buffetaut, G. Escarguel, F. Fluteau, and F. Martineau. Oxygen isotopes from biogenic apatites suggest widespread endothermy in Cretaceous dinosaurs. *Earth and Planetary Science Letters*, 246:41–54, 2006. doi: 10.1016/j.epsl.2006.04.018.

A. Bernard, C. Lécuyer, P. Vincent, R. Amiot, N. Bardet, E. Buffetaut, G. Cuny, F. Fourel, F. Martineau, J.-M. Mazin, and A. Prieur. Regulation of body temperature by some Mesozoic marine reptiles. *Science*, 328(5984):1379–1382, 2010. doi: 10.1126/science.1187443.

B. A. Block. Thermogenesis in muscle. *Annual Review of Physiology*, 56(1):535–577, 1994. doi: 10.1146/annurev.ph.56.030194.002535.

B. L. Bostrom and D. R. Jones. Exercise warms adult leatherback turtles. *Comparative Biochemistry and Physiology Part A: Molecular & Integrative Physiology*, 147(2):323–331, 2007. doi: 10.1016/j.cbpa.2006.10.032.

Y. Cengel. *Heat Transfer: A Practical Approach*. McGraw-Hill Education, 2004. ISBN 9780071236447.

F. Christiansen, S. M. Dawson, J. W. Durban, H. Fearnbach, C. A. Miller, L. Bejder, M. Uhart, M. Sironi, P. Corkeron, W. Rayment, E. Leunissen, E. Haria, R. Ward, H. A. Warick, I. Kerr, M. S. Lynn, H. M. Pettis, and M. J. Moore. Population comparison of right whale body condition reveals poor state of the North Atlantic right whale. *Marine Ecology Progress Series*, 640:1–16, 2020. doi: 10.3354/meps13299.

R. L. Cieri. The axial anatomy of monitor lizards (Varanidae). *Journal of Anatomy*, 233(5):636–643, 2018. doi: 10.1111/joa.12872.

J. Davenport, J. Fraher, E. Fitzgerald, P. McLaughlin, T. Doyle, L. Harman, and T. Cuffe. Fat head: an analysis of head and neck insulation in the leatherback turtle (*Dermochelys coriacea*). *Journal of Experimental Biology*, 212(17):2753–2759, 2009. doi: 10.1242/jeb.026500.

P. N. Dudley, R. Bonazza, and W. P. Porter. Climate change impacts on nesting and internesting leatherback sea turtles using 3D animated computational fluid dynamics and finite volume heat transfer. *Ecological Modelling*, 320:231–240, 2016. doi: 10.1016/j.ecolmodel.2015.10.012.

R. C. Dunkin, W. A. McLellan, J. E. Blum, and D. A. Pabst. The ontogenetic changes in the thermal properties of blubber from Atlantic bottlenose dolphin *Tursiops truncatus*. *Journal of Experimental Biology*, 208(8):1469–1480, 2005. doi: 10.1242/jeb.01559.

F. E. Fish. Biomechanics and energetics in aquatic and semiaquatic mammals: platypus to whale. *Physiological and Biochemical Zoology*, 73(6):683–698, 2000. doi: 10.1086/318108.

C. V. Fleischle, T. Wintrich, and P. M. Sander. Quantitative histological models suggest endothermy in plesiosaurs. *PeerJ*, 6 (e4955), 2018.

FreeCAD. URL https://www.freecad.org. Checked 2025.02.18.

J. Grayson, M. Irvine, and T. Kinnear. Observations on temperature distribution in the cardiovascular system, thorax and abdomen of monkeys in relation to environment. *The Journal of Physiology*, 184(3):581–593, 1966. doi: 10.1113/jphysiol.1966.sp007932.

S. Gutarra and I. A. Rahman. The locomotion of extinct secondarily aquatic tetrapods. *Biological Reviews*, 97(1):67–98, 2022. doi: 10.1111/brv.12790.

S. Gutarra, T. L. Stubbs, B. C. Moon, C. Palmer, and M. J. Benton. Large size in aquatic tetrapods compensates for high drag caused by extreme body proportions. *Communications Biology*, 5:380, 2022. doi: 10.1038/s42003-022-03322-y.

S. F. Hildebrand, C. W. Gilmore, and D. M. Cochran. *Cold-Blooded Vertebrates: Part I. Fishes, Part II-III, Amphibians and Reptiles*, volume 8. Smithsonian Scientific Series, Inc., 1930. URL https://library.si.edu/digital-library/book/coldbloodedverte08hild.

J. E. I. Hokkanen. Temperature regulation of marine mammals. *Journal of Theoretical Biology*, 145(4):465–485, 1990. doi: 10.1016/S0022-5193(05)80482-5.

B. P. Kear. Plesiosaur remains from Cretaceous high-latitude non-marine deposits in southeastern Australia. *Journal of Vertebrate Paleontology*, 26(1):196–199, 2006. doi: 10.1671/0272-4634(2006)26[196:PRFCHN]2.0.CO;2.

E. A. Kiyatkin. Brain temperature and its role in physiology and pathophysiology: Lessons from 20 years of thermorecording. *Temperature*, 6(4):271–333, 2019. doi: doi:10.1080/23328940.2019.1691896.

J. J. Klingler. On the morphological description of tracheal and esophageal displacement and Its phylogenetic distribution in Avialae. *PLoS One*, 11(9):e0163348, 2016. doi: 10.1371/journal.pone.0163348.

T. Kubo, M. T. Mitchell, and D. M. Henderson. *Albertonectes vanderveldei*, a new elasmosaur (Reptilia, Sauropterygia) from the Upper Cretaceous of Alberta. *Journal of Vertebrate Paleontology*, 32(3):557–572, 2012. doi: 10.1080/02724634.2012.658124.

P. H. Kvadsheim, L. P. Folkow, and A. S. Blix. Thermal conductivity of minke whale blubber. 21(2):123–128, 1996. doi: 10.1016/0306-4565(95)00034-8.

J. Lindgren, P. Sjövall, V. Thiel, W. Zheng, S. Ito, K. Wakamatsu, R. Hauff, B. P. Kear, A. Engdahl, C. Alwmark, M. E. Eriksson, M. Jarenmark, S. Sachs, P. E. Ahlberg, F. Marone, T. Kuriyama, O. Gustafsson, P. Malmberg, A. Thomen, I. Rodríguez-Meizoso, P. Uvdal, M. Ojika, and M. H. Schweitzer. Soft-tissue evidence for homeothermy and crypsis in a Jurassic ichthyosaur. *Nature*, 564(7736):359–365, 2018. doi: 10.1038/s41586-018-0775-x.

M. E. Lutcavage, P. G. Bushnell, and D. R. Jones. Oxygen transport in the leatherback sea turtle *Dermochelys coriacea*. *Physiological Zoology*, 63(5):1012–1024, 1990. doi: 10.1086/physzool.63.5.30152626.

F. Menter and T. Esch. Elements of Industrial Heat Transfer Predictions. In *16th Brazilian Congress of Mechanical Engineering*, volume 20, pages 117–127, 2001. ISBN 85-85769-06-6.

F. R. Menter, M. Kuntz, and R. Langtry. Ten Years of Industrial Experience with the SST Turbulence Model. In K. Hanjalić, Y. Nagano, and M. J. Tummers, editors, *Turbulence, heat and mass transfer 4 : proceedings of the Fourth International Symposium on Turbulence, Heat and Mass Transfer*, pages 625–632. Begell House, 2003. ISBN 1567001963.

R. Motani. Swimming speed estimation of extinct marine reptiles: energetic approach revisited. *Paleobiology*, 28(2):251–262, 2002. doi: 10.1666/0094-8373(2002)028%3C0251:SSEOEM%3E2.0.CO;2.

OpenFOAM. URL https://www.openfoam.com. Checked 2025.02.18.

Y. Ouchi, V. S. Chowdhury, J. F. Cockrem, and T. Bungo. Effects of thermal conditioning on changes in hepatic and muscular tissue associated with reduced heat production and body temperature in young chickens. *Frontiers in Veterinary Science*, 7: 610319, 2021. doi: 10.3389/fvets.2020.610319.

F. V. Paladino, M. P. O'Connor, and J. R. Spotila. Metabolism of leatherback turtles, gigantothermy, and thermoregulation of dinosaurs. *Nature*, 344(6269):858–860, 1990. doi: 10.1038/344858a0.

S. V. Petersen, C. R. Tabor, K. C. Lohmann, C. J. Poulsen, K. W. Meyer, S. J. Carpenter, J. M. Erickson, K. K. S. Matsunaga, S. Y. Smith, and N. D. Sheldon. Temperature and salinity of the Late Cretaceous western interior seaway. *Geology*, 44(11):903–906, 2016. doi: 10.1130/G38311.1.

E. R. Price, B. P. Wallace, R. D. Reina, J. R. Spotila, F. V. Paladino, R. Piedra, and E. Vélez. Size, growth, and reproductive output of adult female leatherback turtles *Dermochelys coriacea*. *Endangered Species Research*, 1:41–48, 2004. doi: 10.3354/esr001041.

A. J. Read, W. Keener, M. A. Webber, and U. Siebert. Harbour porpoise *Phocoena phocoena* (Linnaeus, 1758). In Thomas A. Jefferson, editor, *Handbook of Marine Mammals, Coastal Dolphins and Porpoises*, page 427. Academic Press., 2025. doi: 10.1016/B978-0-443-13746-4.00001-9.

M. A. Rogov, N. G. Zverkov, V. A. Zakharov, and M. S. Arkhangelsky. Marine reptiles and climates of the Jurassic and Cretaceous of Siberia. *Stratigraphy and Geological Correlation*, 27:398–423, 2019. doi: 10.1134/S0869593819040051.

T. Sambuichi, U. Tsunogai, and F. Nakagawa. Reconstructing the body temperature of extinct marine reptiles. *Progress in Earth and Planetary Science*, 12:87, 2025. doi: 10.1186/s40645-025-00757-9.

F. J. Schwartz. Behavioral and tolerance responses to cold water temperatures by three species of sea turtles (Reptilia, Cheloniidae) in North Carolina. *Florida Marine Research Publications*, (33):16–18, 1978.

H. B. Stoner. The role of the liver in non-shivering thermogenesis in the rat. *The Journal of Physiology*, 232(2):285–296, 1973. doi: 10.1113/jphysiol.1973.sp010270.

P. Störchle, W. Müller, M. Sengeis, S. Lackner, S. Holasek, and A. Fürhapter-Rieger. Measurement of mean subcutaneous fat thickness: eight standardised ultrasound sites compared to 216 randomly selected sites. *Scientific Reports*, 8(1):16268, 2018. doi: 10.1038/s41598-018-34213-0.

N. Séon, P. Vincent, L. L. Delsett, E. Poulallion, G. Suan, C. Lécuyer, A. J. Roberts, F. Fourel, S. Charbonnier, and R. Amiot. Reassessment of body temperature and thermoregulation strategies in Mesozoic marine reptiles. *Paleobiology*, 51(2):323–343, 2024. doi: 10.1017/pab.2025.2.

R. Tian, T. Zhang, H. Dong, I. Seim, and G. Yang. Cetacean loss of the master adipose tissue regulator β3-adrenergic receptor may underlie their thick blubber and an Oligocene radiation and dispersal. *Nature Communications*, 16:9235, 2025. doi: 10.1038/s41467-025-64288-z.

P. V. Troelsen, D. M. Wilkinson, M. Seddighi, D. R. Allanson, and P. L. Falkingham. Functional morphology and hydrodynamics of plesiosaur necks: does size matter? *Journal of Vertebrate Paleontology*, 39(2):e1594850, 2019. doi: 10.1080/02724634.2019.1594850.

H. K. Versteeg and W. Malalasekera. *An introduction to computational fluid dynamics: the finite volume method*. Pearson Education Limited, second edition, 2007.

J. Wiemann, I. Menéndez, J. M. Crawford, M. Fabbri, J. A. Gauthier, P. M. Hull, M. A. Norell, and D. E. G. Briggs. Fossil biomolecules reveal an avian metabolism in the ancestral dinosaur. *Nature*, 606:522–526, 2022. doi: 10.1038/s41586-022-04770-6.

J. Wiffen, V. de Buffrénil, A. de Ricqlés, and J.-M. Mazin. Ontogenetic evolution of bone structure in Late Cretaceous Plesiosauria from New Zealand. 28(5):625–640, 1995. doi: 10.1016/S0016-6995(95)80216-9.

T. Wintrich, S. Hayashi, A. Houssaye, Y. Nakajima, and P. M. Sander. A Triassic plesiosaurian skeleton and bone histology inform on evolution of a unique body plan. *Science Advances*, 3(12):e1701144, 2017. doi: 10.1126/sciadv.1701144.

J. Wyneken. Anatomy of the Leatherback Turtle. In J. R. Spotila and P. S. Tomillo, editors, *The Leatherback Turtle Biology and Conservation*, pages 34–50. Johns Hopkins University Press, 2015. doi: 10.1353/book.42520.

R. Wéber, D. Gyürki, and Gy. Paál. First blood: An efficient, hybrid one- and zero-dimensional, modular hemodynamic solver. *International Journal for Numerical Methods in Biomedical Engineering*, 39(5):e3701, 2023. doi: 10.1002/cnm.3701.